Publishing House
AKAPIT

COMPUTER METHODS IN MATERIALS SCIENCE

Informatyka w Technologii Materiałów

Vol. 11, 2011, No. 1

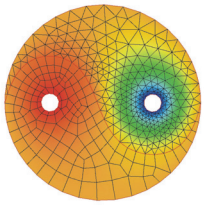

MODELING OF PRIMARY AND EUTECTIC SOLIDIFICATION BY USING CAFD METHOD

ANDRIY BURBELKO*, DANIEL GURGUL

AGH University of Science and Technology, Foundry Faculty
23 Reymonta Str., 30-059 Krakow, Poland
**Corresponding author: abur@agh.edu.pl*

Abstract

The results of a two-dimensional modeling of the microstructure formation in an eutectic ductile cast iron are presented. The cellular automaton model (CA) was used for the simulation. The model takes into account the nucleation of two kinds of grains that appear inside of the liquid during solidification: austenite and graphite.

A numerical solution was used for the modeling of concentration and temperature fields. The parabolic nonlinear differential equations with a source function were solved by using the finite differences method (FD) and explicit scheme. In the interface cells the value of the source function varies depending on the local undercooling. The undercooling value depends on the front curvature, the local temperature and the local chemical composition of the phases. Overlapping lattices with the same spatial step were used for concentration field modeling and for the CA. Another lattice for temperature field was used with a multiple spatial step and the same time step.

The new grain nucleation of solid phases from a liquid is a phenomenon which must be taken into account for correct simulation of a polycrystalline structure formation. An algorithm of continuous nucleation modeling during solidification is presented. The undercooling of solid phase grain nucleation was calculated on the basis of the inverse function of the above cumulative distribution curve (fractile) with the argument equal to the random number generated in the interval 0…1 with uniform density. The domain of correct usage of this algorithm was analyzed.

Key words: cellular automata, solidification, nucleation, cast iron

1. INTRODUCTION

Nodular graphite cast iron – so-called Ductile Iron (DI) – has high mechanical properties in the as-cast state. The properties of such materials can be upgraded as a result of further heat treatment. The microstructure peculiarity of DI is the nodular shape of the grains of one phase – graphite. Another phase that grows directly from the melt during solidification is austenite, a solid solution of carbon in a crystal lattice of γ-Fe. The graphite and austenite grains are nucleated in the direct contact with the melt. At first these grains grow directly from the liquid. Next, the austenite shell encompasses the graphite nodules. This envelope isolates the graphite grains from the liquid phase. From this moment the graphite grains grow due to carbon diffusion from the liquid solution to the nodules' surface through the solid solution layer. The austenite grains still solidify directly from the melt but on the "graphite nodule – austenite envelope" border this phase vanishes and allows spheroid growth.

For direct modeling of the microstructure formation during solidification, two multiscale computational methods are used: the phase-field method (PF) (Karma & Rappel, 1998) and the cellular automata method (CA) (Rafii-Tabar & Shirazi, 2002). Models based on the first one remain to date computationally too costly (Plapp, 2007). The mathematical

 ISSN 1641-8581

model of dendritic solidification of metals and alloys based on the CAFD method (Cellular Automata – Finite Differences) was presented by Umantsev et al. (1985). In CA modeling the outer grain shape and inner structure (e.g. secondary dendrite arm space, solute distribution in the solids, etc.) are the results of the modeling. The following physical phenomenon are taken into account in the modeling: the releasing of the latent heat and heat flow, the redistribution of the solutes and diffusion mass transport as well as Gibbs-Thomson effect. It is possible to take into consideration the non-equilibrium character of the phase transformations. The model's development for one-phase microstructure evolution is the subject of much research: Rappaz & Gandin, 1993, Pavlyk & Dilthey, 2004, Zhu & Hong, 2002, Burbelko at al., 2006. The models of eutectic solidification were presented by Spittle & Brown, 1994 and Zhu at al., 2007, but only for a continuous contact of both growing phases with liquid and for a superimposed temperature condition.

The purpose of the present work is to develop a two-dimensional model to simulate the formation of the DI structure during solidification in a non steady-state temperature condition.

2. A DESCRIPTION OF THE MODEL AND SOLUTION METHOD

The presented model uses a set of six cell states for microstructure modeling: three mono-phase states – "liquid", "austenite", and "graphite" – and three two-phase states. At the beginning, all of the cells in the CA lattice are in the "liquid" state and have eutectic temperature. The liquid phase has eutectic composition (point E in figure 1). The analyzed domain is cooled at a constant cooling rate. When the temperature of the liquid drops below the liquidus, nucleation and growth of the solid grains are possible.

The heterogeneous substrates for the nucleus are randomly distributed in the bulk. The undercooling value of substrate activation is a function of its size. Functional relationship between the active substrate fraction and undercooling ΔT should be a feature of the probability distribution law (Gandin & Rappaz, 1994). The undercooling value of each phase should be calculated relatively to the liquidus lines that are represented in figure 1 by solid lines. The method of continuous nucleation modeling used will be presented in the next part of this paper.

The state of the CA cell with the active nucleus varies from "liquid" to "austenite" or "graphite". The states of adjacent liquid cells are changed to the appropriate interface. The new phase growth and volume fraction changes are only possible in the interface cells.

The kinetic undercooling of the mother liquid phase is a measure of the thermodynamic driving force of the new grains' growth. Total undercooling at the solid-liquid interface (calculated as the difference between the equilibrium solidification temperature T_{Eq} and the real temperature T_r) is equal to the sum of capillary undercooling ΔT_κ and kinetic undercooling ΔT_μ:

$$T_{Eq} - T_r = \Delta T_\kappa + \Delta T_\mu \tag{1}$$

where $\Delta T_\kappa = \Gamma\kappa$, Γ is the Gibbs-Thomson coefficient and κ is a front curvature, which was estimated with the geometrical method proposed by Burbelko, 2004.

The scheme of liquidus lines positions after accounting for the capillary effect for convex grains is shown in figure 1 by dashed lines.

It has been assumed in the computations that the interface migration rate is a linear function of the local kinetic undercooling ΔT_μ:

$$u = \mu \Delta T_\mu \tag{2}$$

where μ is the kinetic growth coefficient.

The increment of the new phase volume fraction in the interface cells Δf over one time step $\Delta\tau$ in the square CA cells of size a was calculated using the equation proposed by Burbelko, 2004:

$$\Delta f = \frac{u\,\Delta\tau}{a\left(|\cos\theta| + |\sin\theta|\right)} \tag{3}$$

where θ is the angle between the X axis and the normal direction of the grain interface.

If the phase volume fraction in the interface cell increases up to 1, this cell varies they state from interface to appropriate one-phase. Additionally, this cell captures all of the adjacent ones: their states exchange to the appropriative interface.

The computer modeling of the heat and mass diffusion processes together with the growing grain shape simulation by the cellular automata method make it possible to predict the structural evolution of the metallic alloy during solidification. The numerical solution of the nonlinear Fourier equation was used for heat flow in the analyzed 2D domain:

$$c\frac{\partial T}{\partial \tau} = \nabla\left(\lambda \nabla T\right) + q_T + q_{cool} \tag{4}$$

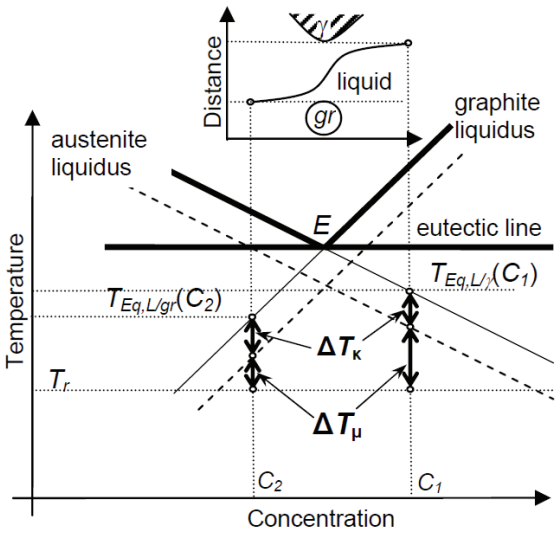

Fig. 1. *Scheme of the stable eutectic region of the Fe-C binary phase diagram:* ΔT_κ *– capillary undercooling,* ΔT_μ *– kinetic undercooling.*

where: T is the temperature, τ is the time, λ is the thermal conductivity, and c is the volumetric specific heat. Two source terms are used: q_{cool} is the intensity of the internal cooling, and q_T is the latent heat generation rate as a consequence of phase transformation.

Solute diffusion in the domains of every phase was calculated separately in the same manner as temperature distribution, by the numerical solution of the diffusion equation:

$$\frac{\partial C}{\partial \tau} = \nabla \cdot (D \nabla C) \tag{5}$$

where D is the solute diffusion coefficient, and C is the solute concentration in this phase.

In the interface cells the following border conditions (opposite in sign for the neighboring grains) was used for the solute redistribution between different phases:

$$q_C = (C_\alpha - C_\beta)\frac{\Delta f}{\Delta \tau} \tag{6}$$

where C_α and C_β are the carbon concentrations in the vanishing and growing phases and Δf is the growth of the new phase volume fraction during the time step.

The carbon concentration in the graphite is always equal to 1. For the "austenite-liquid" interface:

$$C_\gamma = kC_L \tag{7}$$

where k is the solute partition coefficient, and C_γ and C_L are the carbon concentrations in the austenite and liquid.

The equations (4) and (5) were solved by the Finite Differences Method. The implicit scheme was used. The solution to equation (5) was obtained on the dense lattice with the same spatial step as the lattice of CA (overlapped mesh.) The maximum time step of the implicit scheme for the equation (4) solution for the temperature field for this lattice is about 10^4 times shorter. That is why another lattice (the sparse lattice) was used with a multiple spatial step and the same time discretization. The temperature of the interface cells was calculated by linear interpolation from the nodes of the sparse lattice.

Heat source function is equal to zero outside of the interface cells. In the interface cells the value of the heat source for the finite-difference scheme are:

$$q_T = L_{\alpha\to\beta}\frac{\Delta f_\beta}{\Delta \tau} \tag{8}$$

where $L_{\alpha\to\beta}$ is the volumetric latent heat of $\alpha\to\beta$ transformation and Δf_β is the growth of the new phase volume fraction during the time step.

The source function (8) calculated for the cells of the dense mesh was integrated over the area of the elements of the sparse one.

The normal direction of the grain boundary in the interface cells was determined by the approach of the **F**-vector (Dilthley & Pavlik, 1998). The angle θ between the growth direction (normal to the grain boundary) and the positive X-axis direction was calculated as follows:

$$\theta = \arctan\left(\sum_{i,j} y_{i,j} f_{i,j} \Big/ \sum_{i,j} x_{i,j} f_{i,j}\right) \tag{9}$$

where: $f_{i,j}$ is the volume fraction of the phase in the cell (i,j), and $x_{i,j}$ and $y_{i,j}$ are the relative coordinates of the adjacent cells. The summation in (9) concerning the 20 neighboring cells gives the best results of normal direction estimation (Burbelko at al., 2007).

The lines in the binary Fe-C thermodynamic diagram (austenite liquidus, graphite liquidus and carbon solvus line in the austenite) were approximated by a linear function using the data of Kubaschewski, 1985, respectively:

$$T_{Eq,L/\gamma}(C) = 1789.4 - 4076.8\,C - 104589.0\,C^2 \tag{10}$$

$$T_{Eq,L/gr}(C) = -141.5 + 36792.7\,C \qquad (11)$$

$$T_{Eq,\gamma/gr}(C) = 809.1 + 29714.3\,C \qquad (12)$$

The carbon concentration in the above equations is in weight percents.

3. NUCLEATION MODELING

The number of active substrates for nucleation in the domain V of the melt with an undercooling ΔT below the liquidus may be calculated on the basis of the cumulative distribution function $F(\Delta T)$:

$$N = N_{\max} F(\Delta T) V \qquad (13)$$

where: N_{max} is the maximum unit volumetric quantity of substrates for nucleation.

When one substrate position does not have any influence on another substrate's positions, the random variable calculated as the number of substrates in any random domain V will have the Poisson statistical distribution with the mean value $\nu = N_{max}V$. For this statistical distribution the probability density function is:

$$P_r(k) = e^{-\nu}\nu^k / k! \qquad (14)$$

where: e is the Euler-Mascheroni constant and k is the estimated number of substrates.

According to (Gandin & Rappaz, 1994) the undercooling values randomly generated with a statistical distribution curve are attributed to randomly chosen cells. If a cell is chosen several times (i.e. it contains more than one nucleation site), only the smaller nucleation undercooling is used.

If the CA cell is too large, the calculated grain density will be underestimated. A modified version of this algorithm was used in this paper.

First of all, the advisable relation between a cell's volume (or surface for 2D) υ and the substrate density must be estimated. The probability of the lack of a nucleus in the cell ($k = 0$) according to Poisson's statistic is equal to:

$$P_r(k=0) = e^{-\nu} \qquad (15)$$

The probability of one substrate ($k = 1$) in the cell is represented by the following equation:

$$P_r(k=1) = \nu e^{-\nu} \qquad (16)$$

The probability of more than one substrates in one cell may be calculated as:

$$P_r(k>1) = 1 - e^{-\nu}(1+\nu) \qquad (17)$$

For the small ν $e^{-\nu} \approx 1-\nu$, we will hereby use the following equation:

$$P_r(k>1) = \nu^2 \qquad (18)$$

The mean number of cells in a CA lattice with M_{CA} cells where more than one substrate is located is equal to $M_{CA}\cdot\nu^2$. Because $\nu = N_{max}\cdot\upsilon$, the next criterion may be proposed for an estimation of the correct nucleation model using:

$$M_{CA}(N_{max}\upsilon)^2 < K \qquad (19)$$

When the above inequality is true, the mean number of cells in a CA lattice where more than one substrate is present will be less than K.

The following way of substrate placement and the undercooling of nucleation selection is proposed based on the mean number of active substrates in one cell:

$$\nu = N_{max} F(\Delta T)\upsilon \qquad (20)$$

For each of the cells in the CA a random number p should be generated with an equiprobability distribution in the $\langle 0..1\rangle$ range. The condition of the substrate present in the cell is the following inequality:

$$p < N_{max} F(\Delta T)\upsilon \qquad (21)$$

The nucleation undercooling in this case should be estimated on the basis of the inverse function of the above-mentioned cumulative distribution curve (fractile):

$$\Delta T = F^{-1}(p) \qquad (22)$$

The solid grain will begin to grow when the undercooling exceeds the above level. The substrates are present (and nucleation is possible) only in cells with a positive ΔT value.

The Weibull statistical distribution was used in this paper for nucleation modeling. The specific number of active substrates was given by Fraś at al., 2001

$$n = N_{\max} \exp(-b/\Delta T) \qquad (23)$$

where b is a nucleation coefficient.

The undercooling of nucleation can be calculated as:

$$\Delta T = -b \Big/ \ln\left(\frac{p}{\upsilon N_{\max}}\right) \qquad (24)$$

The values for N_{max} and b used in the present work for the modeling of graphite and austenite grains nucleation are listed in table 1.

Table 1. *Nucleation parameters.*

	Austenite	Graphite
b, K	5	300
N_{max}, m^{-2}	$1.5 \cdot 10^7$	$1.0 \cdot 10^9$

4. RESULTS OF COMPUTATIONS

Computations were carried out on a grid of 640×640 cells. The side of each cell was 1 μm in length. An initial uniform carbon concentration in the binary Fe-C liquid was assumed equal to 0.0425 part of the mass fraction (eutectic concentration). Basing on Kubaszewski, 1985, k_C = 0.49 was adopted as the equilibrium coefficient of carbon distribution between the liquid phase and austenite. Other thermo-physical parameters that are used in the modeling are typical for Fe-C alloy of eutectic composition (see Burbelko at al., 2010).

For thermal conditions in the computational region, the following boundary conditions were adopted: at the top of the grid – an adiabatic condition, at the bottom of the grid – a boundary condition of the third type, at the sides of the region – a periodic boundary condition described by Burbelko, 2004. For the carbon concentration field on the side boundaries of the region, a periodic boundary condition was adopted, for the top and bottom – an absence of mass flow. Simulation was performed for the internal cooling rate (q_{cool} /c) equal to -10 K/s.

The results of the modeling are presented in figure 2. All of the graphite grains in this figure are shown in the same color. The austenite grains have a different level of gray (constant for each grain). The gray level in the liquid domain shows the carbon concentration.

As graphite nodules, austenite dendrites nucleate from the liquid. During crystallization from the liquid phase ahead of the austenite growth front, a liquid zone rich in carbon is formed. The solubility of carbon in the growing solid phase is lower than in the disappearing liquid phase. A reverse situation occurs in the liquid ahead of the front of graphite growth. In places where the distance between the growing phases is not large enough, a soft collision occurs therefore the concentration fields start acting on the growing grains, destroying the symmetry of their growth. If this collision occurs in the case of two identical grains (austenite-austenite or graphite-graphite), their growth will be arrested in the direction of the collision. The soft collision of grains of different phases – provided a phase rich in carbon, e.g. graphite, appears near the growing austenite grain – accelerates carbon diffusion in the direction between the phases. In this case, carbon concentration decreases ahead of the austenite grain growth front, and increases ahead of the graphite growth front. The concentration gradient of the dissolved constituent increases, resulting in accelerated diffusional mass transport. At the same time, with the above-mentioned changes of the concentration profile in the liquid phase, undercooling increases

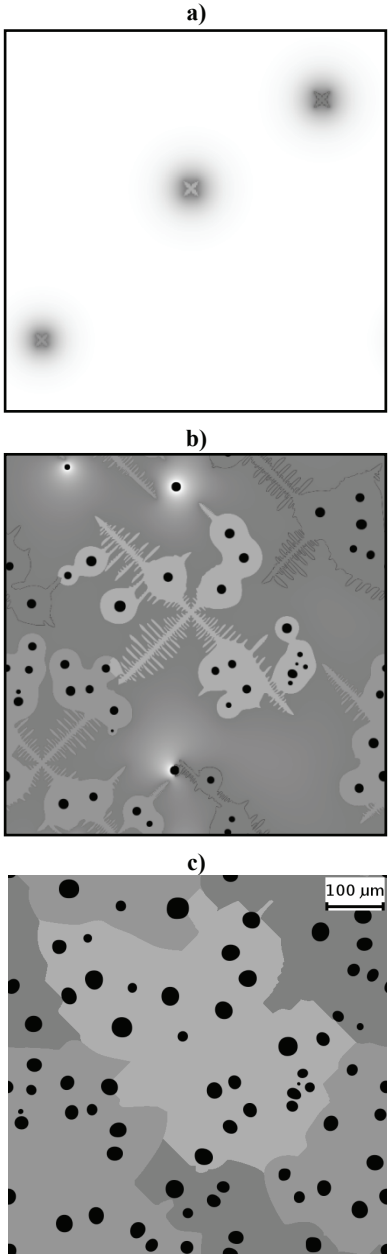

Fig. 2. *The stages of DI microstructure formation (modeling); time, s: a) 2; b) 17; c) 48*

at both solidification fronts. The thermodynamic driving force of the crystallization of both phases increases, resulting in accelerated migration of the grain boundaries towards one another. The scheme of carbon distribution in the liquid between the austenite and graphite grains (with a non-equilibrium border concentration on both interfaces) is shown at the top part of figure 1. Example of the real microstructure of industrial ductile iron and graphite particle distribution is presented in figure 3.

Obtained results are in the good correlation with the experimental investigation of solidification structure of DI developed by Rivera at al., 2002, 2008 with using the EBSD method: each austenite grain has non-regular borders and can cover several graphite nodules.

The history of mean temperature changes in the analyzed domain obtained in the simulation is presented in figure 4. Presented cooling curve qualitatively is similar to the experimental one received by Kapturkiewicz at al., 2010 for the eutectic ductile iron.

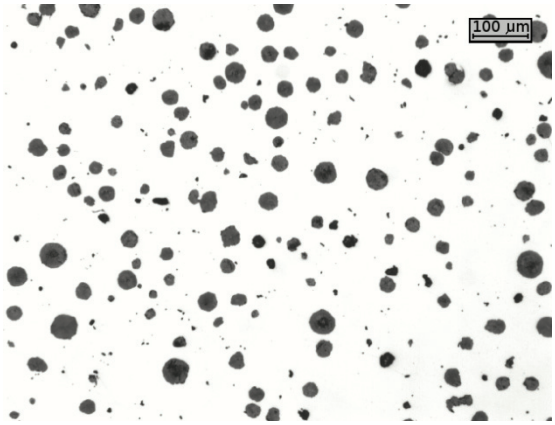

Fig. 3. *Real microstructure of DI, non-etched*

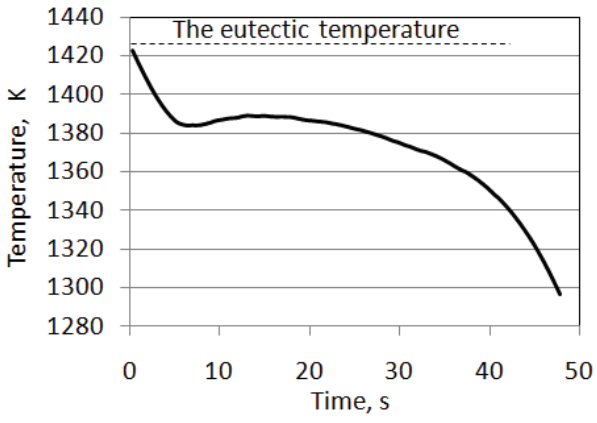

Fig.4. *Cooling curve, modeling.*

5. CONCLUSIONS

The results of the simulation of the initial stage of growth of austenite dendrites and graphite nodules in cast iron have been presented. The results have been obtained using the authors' own computational program.

It has been proved that the rate of growth of the austenite dendrite branches can increase during simulation if a grain of graphite is placed nearby.

After the enclosing of the graphite nodules by austenite, further growth of the graphite is possible because carbon diffuses from the liquid solution to the nodules' surface through the solid solution layer.

It has been shown that each austenite grain can cover several graphite nodules. These results are in good correlation with the experimental investigation.

ACKNOWLEDGMENTS

This study was performed under Polish MNiSW Project No. N507 422536.

REFERENCES

Burbelko, A., Gurgul, D., Fraś, E., Guzik, E., 2010, *Multiscale modeling of ductile iron solidification with continuous nucleation by a cellular automaton*, 30th Computers and Information in Engineering Conference.

Burbelko, A., 2004, *Mezomodeling of Solidificatnion Usin a Cellular Automaton*, UWND AGH, Krakow (in Polish).

Burbelko, A.A., Fraś, E., Kapturkiewicz, W., Olejnik, E., 2006, Nonequilibrium Kinetics of Phase Boundary Movement in Cellular Automaton Modelling, *Materials Science Forum*, 508, 405-410.

Burbelko, A.A., Kapturkiewicz, W., Gurgul, D., 2007, Analysis of causes and means to reduce artificial anisotropy in modelling of the solidification process on cellular automaton, Solidification Processing 2007: *Proceedings of the 5th Decennial International Conference on Solidification Processing*. H. Jones eds., The University of Sheffield, UK, 2007, 31-35.

Dilthley, U., Pavlik, V., 1998, Numerical simulation of dendrite morphology and grain growth with modified cellular automata, *Modeling of Casting, Welding and Advanced Solidification Processes VIII*, B.G. Thomas and C. Beckermann eds., TMS, Warrendale, 1998, 589-596.

Fraś, E., Wiencek, K., Górny, M., Lopez, H., 2001, Nucleation and grains density - a theoretical model and experimental verification, *Archives of Metallurgy*, 46(3), 317-322.

Gandin, Ch.-A., Rappaz, M., 1994, "A Coupled Finite Element-Cellular Automaton Model for The Prediction Of Dendritic Grain Structures in Solidification Processes", Acta metall. mater., 42(7), 2233-2246.

Kapturkiewicz, W., Burbelko, A.A., Fraś, E., Górny, M., Gurgul, D., 2010, Modelling of ductile iron solidification using the cellular automaton and finite differences method, *Polish metallurgy 2006-2010 in time of the worldwide economic crisis*, eds, K. Świątkowski, L. Blacha, J.

Dańko, M. Pietrzyk, J. Dudkiewicz, J. Kazior; Committee of Metallurgy of the Polish Academy of Science, Akapit, Kraków, 99-122.

Karma, A., Rappel, W.-J, 1998, Quantitative phase-field modeling of dendritic growth in two and three dimensions, *Phys. Rev. E*, 57(4), April, 4323-4349.

Kubaschewski, O., 1985, *Iron – Binary Phase Diagrams*, Springer-Verlag, Berlin.

Pavlyk, V., Dilthey, U., 2004, Simulation of Weld Solidification Microstructure and its Coupling to the Macroscopic Heat And Fluid Flow Modelling, *Modelling and Simulation in Materials Science and Engineering*, 12(1), S33-S45.

Plapp, M., 2007, Three-dimensional phase-field simulations of directional solidification, *Journal of Crystal Growth*, 303, 49-57.

Rafii-Tabar, H., Chirazi, A., 2002, Multi-scale computational modelling of solidification phenomena, *Physics Reports-Review Section of Physics Letters*, 365(3), 145-249.

Rappaz, M., Gandin, Ch.A., 1993, Probabilistic Modeling of Microstructure Formation in Solidification Processes, *Acta Metallurgica et Materialia*, 41(2), 345-360.

Rivera, G., Boeri, R., Sikora J., 2002, Revealing and characterising solidification structure of ductile cast iron, *Materials Science and Technology*, 18(7), 691-697.

Rivera, G., Calvillo, P.R., Boeri, R., Houbaert Y., Sikora J., 2008, Examination of the solidification macrostructure of spheroidal and flake graphite cast irons using DAAS and ESBD, *Materials Characterization*, 59, 1342-1348.

Spittle, J.A., Brown, S.G.R., 1994, A 3D Cellular Automaton Model of Coupled Growth in Two Component Systems, *Acta Metall. Mater*., 42(6), 1811-1815.

Umantsev, A.R., Vinogradov, V.V., Borisov, V.T., 1985, Mathematical Modeling of the Dendrite Growth in the Undercooled Melt, *Kristallografia*, 30(3), 455-460. (In Russian)

Zhu, M.F., Hong, C.P., Stefanescu, D.M., Chang, Y.A., 2007, Computational modeling of microstructure evolution in solidification of aluminum alloys, *Metall. Mater. Trans. B*, 38B(4), 517-524.

Zhu, M.F.; Hong, C.P., 2002, A Three Dimensional Modified Cellular Automaton Model for the Prediction of Solidification Microstructures, *ISIJ International*, 42(5), 520-526.

MODELOWNIE KRYSTALIZACJI FAZY PIERWOTNEJ I EUTEKTYKI METODĄ CAFD

Streszczenie

Przedstawiono wyniki dwuwymiarowego modelowania procesu tworzenia się mikrostruktury eutektycznego żeliwa z grafitem kulkowym. W pracy wykorzystano model oparty na metodzie automatu komórkowego (CA od ang. Cellular Automaton). W modelu uwzględniono zarodkowanie ziaren dwu faz z cieczy podczas krystalizacji: grafitu i austenitu pierwotnego.

Dla modelowania pola stężenia i temperatury wykorzystuje się rozwiązania numeryczne. Rozwiązanie parabolicznego nieliniowego równania różniczkowego z funkcją źródła uzyskuje się metodą różnic skończonych (FD od ang. Finite Differences) ze schematem jawnym. Wartość funkcji źródła w komórkach interfejsu zależy od lokalnego przechłodzenia na froncie krystalizacji. Wartość przechłodzenia jest wyznaczana z uwzględnieniem krzywizny granicy międzyfazowej na podstawie lokalnej temperatury i temperatury równowagi fazowej zależnej od lokalnego składu chemicznego cieczy. W modelowaniu stężenia wykorzystano nakładające się siatki FD i CA z identycznym krokiem. W modelowaniu pola temperatury zastosowano rzadką siatkę z wielokrotnym krokiem przestrzennym i identycznym krokiem czasowym.

Dla poprawnego modelowania struktury materiałów polikrystalicznych należy uwzględnić zjawisko zarodkowanie ziaren stałych z fazy ciekłej. Opisano algorytm modelowania ciągłego zarodkowania nowych ziaren podczas krystalizacji. Przechłodzenie, przy którym powstają zarodki ziaren nowych faz, jest obliczane na podstawie odwrotnej funkcji do dystrybuanty (kwantyl) rozkładu statystycznego Weibulla i liczb pseudolosowych o rozkładzie jednostajnym w zakresie 0...1. Przeanalizowano zakres poprawnego wykorzystania tego algorytmu.

Received: October 11, 2010
Received in a revised form: December 12, 2010
Accepted: December 14, 2010